Advancing Squarewave Voltammetry at PEDOT/fCNT Carbon Fiber Microelectrodes for In Vivo Basal Dopamine Detection

by

Noah Chaim Freedman

Bachelor of Science in Bioengineering, University of Pittsburgh,

2019

Submitted to the Graduate Faculty of

the University Honor's College in partial fulfillment

of the requirements for the degree of

Bachelor of Philosophy

University of Pittsburgh

2019

UNIVERSITY OF PITTSBURGH

DEPARTMENT OF BIOENGINEERING

This thesis was presented

by

Noah Chaim Freedman

It was defended on

April 16, 2019

and approved by

Tracy Xinyan Cui, PhD, University of Pittsburgh Department of Bioengineering

Ian Mitch Taylor, PhD, Saint Vincent College Department of Chemistry

Elisa Castagnola, PhD, University of Pittsburgh Department of Bioengineering

Adrian Michael, PhD, University of Pittsburgh Department of Chemistry

Takashi Kozai, PhD, University of Pittsburgh Department of Bioengineering

Thesis Advisor: Tracy Xinyan Cui, PhD, University of Pittsburgh Department of Bioengineering

Copyright © by Noah Chaim Freedman
2019

Advancing Squarewave Voltammetry at PEDOT/fCNT Carbon Fiber Microelectrodes for In Vivo Basal Dopamine Detection

Noah Chaim Freedman, B.Phil

University of Pittsburgh, 2019

Dopamine is a central nervous system neurotransmitter responsible for vital human functions which operates via two signalling modes. Phasic signalling comprises subsecond fluctuations in extracellular DA, whereas tonic signalling comprises minute to hour fluctuations. Both signalling modes are critical to study for full characterization of a given *in vivo* DA system, but currently available methods for sampling tonic signalling possess significant limitations, including limited spatial resolution and extensive damage upon implantation among others. In order to provide an alternative electrochemical detection technique for the quantification of tonic *in vivo* DA signalling, squarewave voltammetry (SWV) has been developed at carbon fiber electrodes (CFEs), but has suffered issues of low DA sensitivity and extensive signal interferences from electrochemically active analytes such as ascorbic acid (AA). Thus, a surface coating of poly(3,4-ethylenedioxythiophene) with carboxy-functionalized carbon nanotubes (PEDOT/fCNT) has been developed for implementation on CFE substrates to increase DA sensitivity. Persistent issues preventing reliable *in vivo* application of this technology include extensive AA interference and significant discrepancies between conditions of the *in vitro* calibration environment and *in vivo* recording environment. The latter issue generalizes to all electrochemical sensing techniques. It was hypothesized that PEDOT/fCNT coatings and the introduction of 0 V static potential periods prior to SWV application may be implemented as strategies to mitigate AA interference. Furthermore, agarose gels and bovine serum albumin surface adsorption were explored as potential mechanisms through which *in vitro* conditions may more closely approximate the *in vivo* for more reliable calibrations and data interpretation. PEDOT/fCNT was found to significantly increase AA sensitivity, decrease relative DA to AA peak amplitude, and increase the redox profile separation between AA and DA in the SWV ΔI trace. 0 V static potential application demonstrated ability to significantly reduce AA peak amplitude while simultaneously increasing DA peak amplitude

without exhibiting significant effects on sensitivity. Finally, agarose gel and protein adsorption strategies were unsuccessful in replicating *in vivo* conditions *in vitro*, but point to future methods by which this goal may be achieved. This work represents a major step forward in realizing a powerful basal DA sensing tool for the neurosciences and bioengineering.

Table of Contents

List of Figures

1.0 Introduction

Dopamine (DA) is a monoamine neurotransmitter of the central nervous system (CNS) which undergoes vesicular release and active transporter reuptake at the synaptic bouton [1]. The importance of DA neurotransmission in the CNS has been established for many vital functions including pleasure and reward motivated behaviors, motor control, and hormonal regulation among others [2, 3, 4]. In mediating these functions, DA signaling occurs through two primary modes: phasic and tonic signalling. Phasic signaling comprises sub-second fluctuations in extracellular (EC) DA arising out of singular neurotransmission events and rapid changes in neural activity, and is implicated in learning, controlling conditioned stimuli, drug abuse and appetitive behaviors [2, 5, 6]. In contrast, tonic signaling arises from slow modulations in the basal dopaminergic neural firing rate which induce fluctuations in the local EC DA concentration on minute to hour timescales. Tonic signaling mediates phasic signaling, and is involved in motor control and higher order cognitive functions [7, 8]. Furthermore, dysregulation of phasic and tonic DA signaling is implicated in major depressive disorder, schizophrenia, substance abuse disorder, attention-deficit/hyperactivity disorder and Parkinsons disease among others [9, 10, 11, 12]. Therefore, it is essential to consider both phasic and tonic signaling in the neurochemical study of CNS DA sytems for uncovering the neurochemical bases of natural human functions and disease pathologies.

A direct approach for quantifying phasic and tonic signals for DA system characterization *in vivo* generally comprises measuring the EC concentration of DA in a local cerebral region over time. Alhough various methods have been devised for direct measurement of both tonic and phasic concentration profiles in the brain, there remains a strong need for an improved *in vivo* tonic DA measurement technique due to the shortcomings of leading methodologies.

1.1 Current In Vivo Basal Dopamine Detection Methods

1.1.1 Microdialysis

Microdialysis was introduced in the 70s by Delgado, Ungerstedt and Pycock as a tool for sampling extracellular analytes in the CNS and was the first method used to quantify tonic DA signals *in vivo* [13, 14]. The essential system remains relatively unchanged and comprises three components: the microdialysis probe, the perfusate, and the *ex vivo* analysis technique. Microdialysis probes are typically 4 mm in length and 220 μM in outer diameter, possessing an inlet channel through the center of the probe, a semipermeable membrane covering most of the outer surface area, and an outlet channel which collects perfusate that has passed along the inner wall of the membrane. Once implanted into the CNS, the probe is perfused with artificial cerebrospinal fluid at a rate of 0.3-3 μL/min and the outlet perfusate is collected every 1-20 min [15, 16]. During perfusion, analytes adjacent the dialysis membrane diffuse into the perfusate driven by concentration gradient. Once the outlet perfusate is collected, compositional analysis may be performed to determine analyte concentration by any one of many established techniques including liquid chromatography, microchip electrophoresis, UV analysis, fluorescence, electrochemical detection, mass spectroscopy, and nuclear magnetic resonance [17, 18, 19, 20, 21].

At present, microdialysis sample quantifications may be performed with a maximum temporal resolution of 1 min, preventing phasic DA monitoring but preserving the ability to measure tonic signals. However, due to difficulties in accounting for diffusion differences at the membrane interface between *in vitro* and *in vivo* environments, and the dependence on *in vitro* calibrations for *in vivo* data interpretation, quantifications are typically reported in the form of differentials from an initially measured baseline signal [22, 23]. This greatly limits the power of this technique, as absolute basal [DA] is not easily accessible. Furthermore, large probe dimensions prevent sampling at high spatial resolution and induce significant tissue damage upon implantation, exacerbated by the relatively small CNS blood vessel spacing of 60 μM [23, 24]. Substantial implantation injury confounds DA measurement by perturbing the local neural tissue and it has been demonstrated that the implantation injury

of microdialysis is significantly larger than other techniques which utilize smaller probes [24]. Additionally, the tissue response to implantation injury typically limits chronic microdialysis studies to within 10 days, rendering this technique unsuitable for monitoring long-term neurochemical changes throughout disease progression [22, 25].

1.1.2 Fast-Scan Controlled Adsorption Voltammetry

Fast-scan controlled adsorption voltammetry (FSCAV) is a recently developed electrochemical technique for basal DA quantification [26]. If subjected to sufficiently high and low voltage in rapid sequence, DA may undergo undergo reversible oxidization and reduction reactions, passing through the intermediate molecule dopamine-o-quinone (Fig. 1). Through

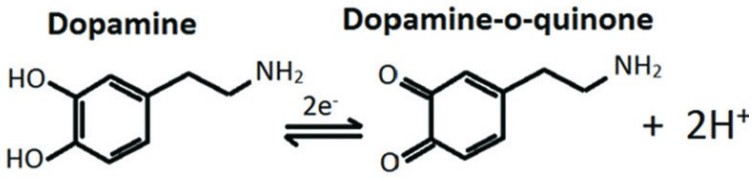

Figure 1: Dopamine oxidation to dopamine-o-quinone, and the reverse reduction reaction.

the reduction and oxidation (redox) reactions, DA exchanges a pair of electrons with the oxidizing and reducing substrate. FSCAV exploits this phenomenon via implanting a conducting carbon-fiber microelectrode (CFE, Fig. 2) into the brain and controlling the voltage of the electrode while measuring the electrode current. Thus, the electrode serves as the redox substrate and redox currents may be measured as electrons are exchanged. The working principles of FSCAV may be best understood by first briefly touching upon fast-scan cyclic voltammetry (FSCV), an electrochemical technique upon which it is based.

In a traditional method of phasic DA quantification known as fast-scan cyclic voltammetry (FSCV), an increasing then decreasing triangle voltage waveform is applied at a CFE while electrode current is measured [27]. CFEs possess high surface affinity for DA adsorption, facilitating accumulation of ambient DA to the electrode surface such that measured redox currents, also known as faradaic currents, may be enhanced. However, faradaic currents are masked by simultaneously induced capacitive currents, or non-faradaic currents, as the

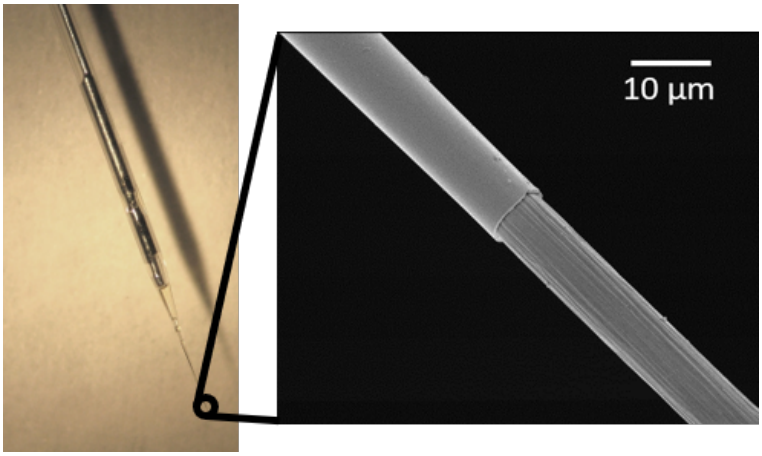

Figure 2: Bare CFE for *in vivo* FSCAV and FSCV DA measurement. Typical dimensions of the exposed electrically active portion of the fiber are 7 μm by 400 μ

CFE repeatedly charges and discharges with electrochemically inactive ionic species. To isolate DA redox signals for quantification, a reference scan is subtracted possessing a similar capacitive current profile, typically collected shortly before the scan of interest [28]. Due to the unstable nature of background non-faradaic currents over time and the inability of FSCV to measure [DA] in an isolated scan, this technique may not be applied for tonic DA characterization and is limited to differential phasic DA detection [29]. However, FSCAV overcomes this limitation by utilizing a modified voltage waveform sequence.

The FSCAV measurement begins with a brief period of 100 Hz FSCV application to minimize DA adsorption to the CFE surface. This is followed by a prolonged period of -0.4 V static application, inducing controlled DA-adsorption to the CFE surface such that adsorption equilibrium is reached with a final surface content proportional to the bulk concentration. Finally, a second round of 100 Hz FSCV is performed to monitor redox activity as DA diffuses away from the surface until a new adsorption equilibrium is reached. To quantify the local basal DA concentration, DA redox currents are isolated throughout the FSCV diffusion period using reference scans from the initial FSCV DA minimization period. Redox signals are then integrated across all scans to obtain a final charge metric which correlates linearly with local DA concentration *in vitro*. This scanning procedure may be repeated every 20 s,

achieving final temporal and spatial resolutions for basal tonic DA signaling quantification greater than those of microdialysis (CFE dimensions addressed in Fig. 2) [26]. Successful *in vivo* FSCAV measurements have since been performed for basal DA quantification in the mouse nucleus accumbens [30].

As FSCAV depends extensively on the DA adsorption properties of CFEs, it is unclear if this method may be adapted for a non-carbon-based electrode platform, such as those typically used for constructing metal-based multiple electrode arrays (MEAs). Although carbon fiber shank arrays have been demonstrated, lithographically fabricated metallic site MEAs provide a significant advantage with regards to fabrication ease and spatial resolution [31, 32]. Thus, FSCAV is presently limited in its ability to resolve tonic signals with high spatial resolution. Additionally, FSCAV is subject to electrochemical interference from the electrochemically active molecules norepinephrine (NE) and dopac (DO) which exhibit redox profiles throughout a scan which significantly overlapping with the characteristic DA signal [33]. Therefore, DA measurement via FSCAV is further limited to applications in brain regions with low concentrations of these molecules such as the dorsal striatum.

1.2 Foundations of a Novel DA Sensing Platform

Microdialysis and FSCAV presently comprise the most reliable methods of basal DA quantification, yet each are subject to significant limitations as previously described. There remains a need for a selective detection method capable of resolving *in vivo* basal DA signals with high temporal and spatial resolution, and which may be implemented on metallic MEA substrates for enhanced spatial information. To address this persistent need, a novel *in vivo* DA sensing platform has been developed, exhibiting high sensitivity for basal DA, high DA selectivity over other physiologically present electrochemically active analytes, and which has demonstrated feasibility for use at lithographically fabricated MEAs in prelimiary work. The detection method is based on the electrochemical technique of squarewave voltammetry (SWV), developed by the Osteryoungs in 1985 [34], and a highly conductive polymer nanocomposite electrode coating of poly(3,4-ethylenedioxythiophene)

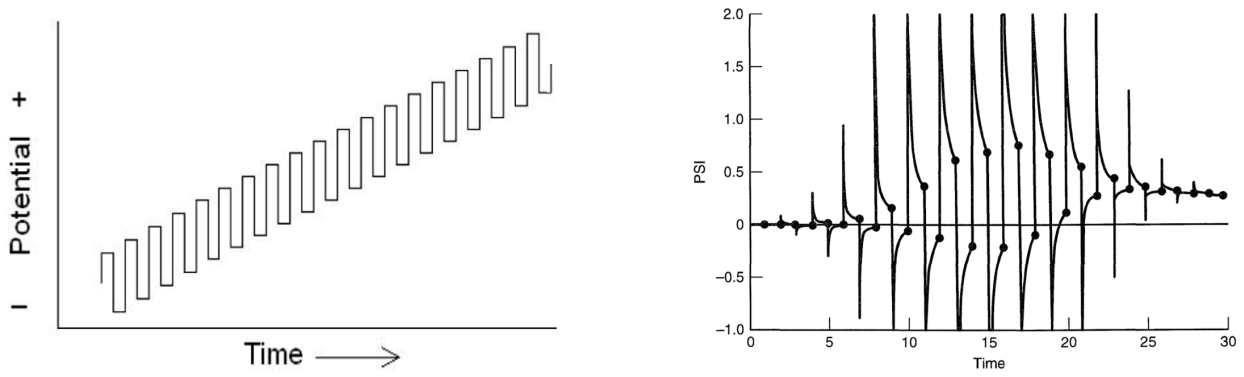

(a) (b)

Figure 3: A single scan of a generic SWV voltage waveform (a) and dimensionless current traces from theoretical analysis of a particular waveform instatiation (b).

with carboxyl-functionalized carbon nanotubes. The primary functions of each component will be addressed in the following subsections.

1.2.1 Squarewave Voltammetry

SWV is a voltammetric technique designed to sample faradaic currents in relative isolation from non-faradaic currents at a particular voltage. Measuring faradiac currents are of primary concern given the desire to obtain information regarding the concentration of an electrochemically active species. In a voltammetric scheme, information relevant to analyte concentration is contained in the faradaic component of the sampled current, and quantification techniques are typically designed to analyze this component separate from confounding background non-faradaic currents. SWV is capable of resolving faradaic signals in near-isolation from non-faradaic signals by applying a particular voltage waveform comprising the summation of a stairstep and a squarewave (Fig. 3a), and a modified version of this waveform termed multiple-cyclic SWV has been successfully used for tonic DA measurement at PEDOT/nafion coated CFEs [35].

One may usefully conceptualize this waveform by considering a series of symmetric cathodic

and anodic square voltage pulses, in which a subsequent pair of pulses is centered at a slightly higher voltage specified in the waveform design. During a single positive or negative pulse, the non-faradaic electrode current decays exponentially while the faradiac current decays according to an inverse polynomial [36]. SWV leverages this property by sampling the current at the end of each pulse, such that the proportion of the non-faradaic current in the measured signal is minimized (Fig. 3b). Furthermore, for each pair of pulses, the 2 sampled currents are combined by subtracting the anodic pulse current from the cathodic pulse current, resulting in a final signal with a single current value per centered voltage referred to as ΔI. Therefore, for a given pulse pair, all electrochemically active analytes possesing redox currents lying between the cathodic and anodic potentials will be oxidized and then then reduced. Subsequently, as the waveform passes the redox potential of a particular electrochemically active analyte, ΔI increases, reaches a maximum value, and then decays as the oxidization equilibrium is reached [36]. In the presence of DA, this redox process manifests as a peak in the ΔI trace at approximately 0.15 V which may be quantified and correlated with a local concentration via calibration.

Due to the relatively high impedance of small electrode sites and intrinsically low currents associated with this technique, typical *in vivo* electrochemical sensing electrodes, such as CFEs, are not suitable for sensitive application of SWV. However, CFEs represent the most suitable substrate for implementating SWV for DA detection, as these electrodes have been well established for the detection of DA in the field of *in vivo* neurochemical sensing due to their high affinity for DA adsorption and sensitivity to redox events compared to other electrodes [26, 27, 28, 29, 30, 31, 32, 33, 36]. Thus, in order to successfully realize SWV at implantable microelectrodes, it was necessary to investigate methods of electrode modification to overcome issues of high impedance.

1.2.2 PEDOT/fCNT

It was hypothesized that the highly conductive nanocomposite poly(3,4-ethylenedioxythiophene) with carboxy functionalized carbon nanotubes (PEDOT/fCNT) may be deposited onto the electrode surface to achieve decreased electrode impedance and in turn

increase DA sensitivity via SWV detection (Fig. 4). Previous work has shown that PEDOT/fCNT surface coatings significantly reduce 1 kHz impedance at PtIr electrophysiological sensors, resulting in greater electrical sensitivity, and furthermore endow enhanced stability and biocompatibility over the course of chronic *in vivo* electrophysiological recordings [37, 38]. Thus, PEDOT/fCNT was considered a suitable candidate for overcoming impedance restrictions on SWV at CFEs and for eventual biocompatibility for future chronic *in vivo* applications. PEDOT/fCNT may be successfully and controllably deposited via chronocoulom-

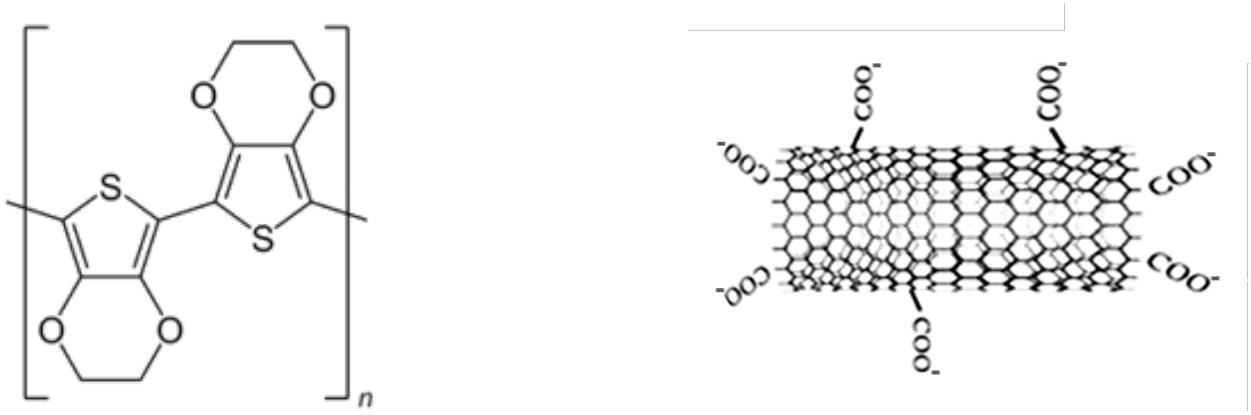

(a) (b)

Figure 4: (a) PEDOT polymer unit and (b) basic fCNT structure. fCNTs utilized in this study are multiwalled and possess carboxylated surfaces.

betric electropolymerization onto the surface of CFEs for significantly decreased electrochemical impedance (Fig. 5a-c, see methods for details). As predicted, decreased impedance directly translated to enhanced DA detection sensitivity via SWV, assessed through performing *in vitro* DA calibrations (Fig. 5d, see methods for details). Enhanced sensitivity enabled successful *in vivo* basal DA detection in the rat dorsal striatum at PEDOT/fCNT coated CFEs, and preliminary work has suggested that this platform may be implemented at lithographically fabricated metal-site MEAs as well for multi-site *in vivo* recordings. Thus, this technique holds promise for providing a powerful basal DA-sensing tool which may circumvent the shortcomings of microdialysis and FSCAV.

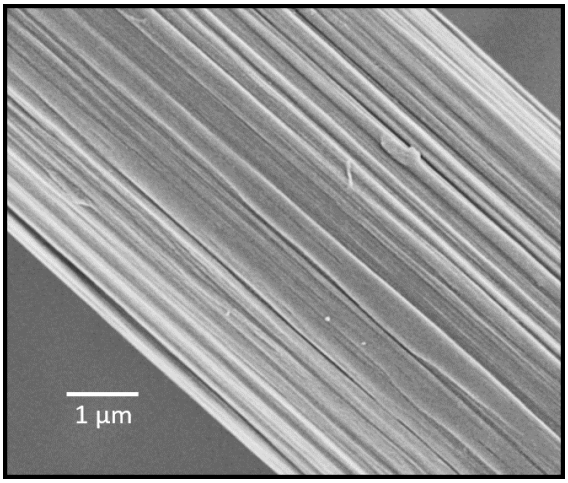

(a)

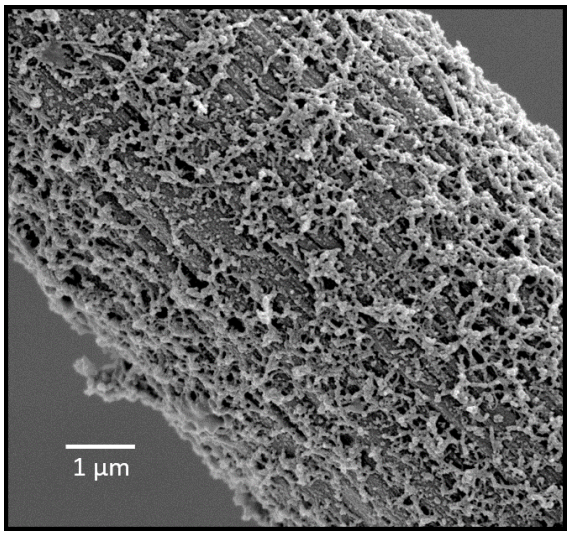

(b)

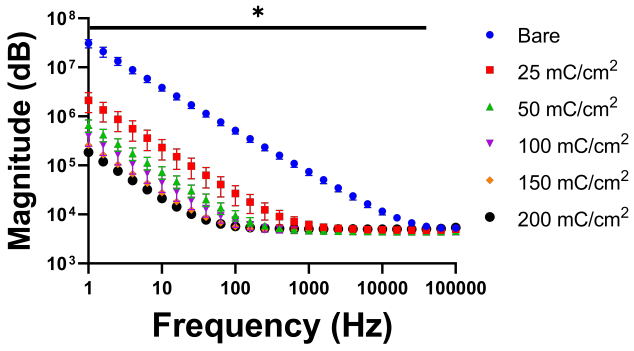

(c)

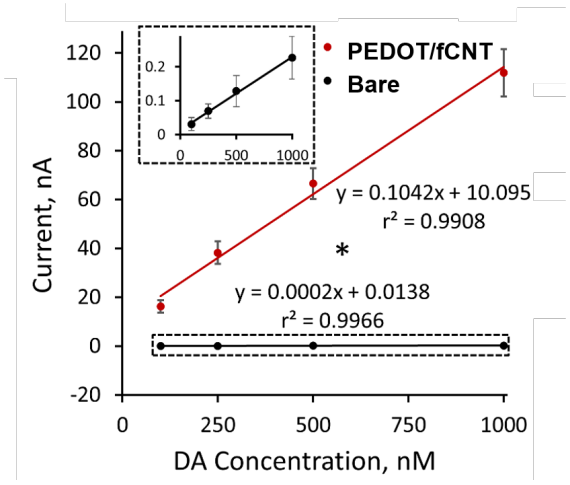

(d)

Figure 5: (a) Bare CFE surface and (b) 25 mC/cm^2 PEDOT/fCNT coated CFE surface as viewed under scanning electron microscope. (c) PEDOT/fCNT at various charge densities significantly decreases *in vitro* electrode impedance magnitude. $*$ indicates $p < 0.005$. (d) Increased PEDOT/fCNT coating results in increased *in vitro* DA sensitivity. $*$ indicates $p < 0.05$.

2.0 Objective

This thesis will address critical developments in mitigated two of the primary issues confounding application of SWV at PEDOT/fCNT CFEs for *in vivo* basal DA measurement. Methods for attenuating signal interference from the most prominent electrochemically active molecule in the CNS will be addressed, followed by a review of progress in developing an improved platform for *in vitro* calibrations to enable more reliable interpretation of *in vivo* recordings.

2.1 AA Signal Interference

DA measurements via SWV are subject to electrochemical interference in cases where other electrochemically active molecules are present. As SWV is not an inherently selective technique, electrochemically active molecules possessing redox potentials within the boundaries of the scan will contribute to the measured signal according to their redox profile. Redox profiles may overlap and in some cases result in a final ΔI trace in which the presence of two distinct redox profiles is not apparent. Since the extent of signal quantification using SWV analysis comprises measuring the amplitude of the current peak produced by the redox activity of a given analyte, significant overlap can completely confound quantification of either analyte.

In the case of DA detection, the most prominent molecule which exhibits significant interference is acsorbic acid (AA), an antioxidant present *in vivo* at concentrations approximately three orders of magnitude greater than that of DA ($\sim$O(100μM) AA vs. $\sim$O(100nM DA)) [39, 40]. Early *in vitro* investigations of potential interference effects from AA on the DA redox signal during SWV at bare CFEs revealed masking of the DA signal sufficient to completely hinder reliable quantification (Fig. 6). Given comparable conditions *in vivo*, this effect, combined with previously described low sensitivity issues, fully prevents application of SWV at bare CFEs for basal DA measurement.

The first objective of this thesis is to provide a comprehensive analysis of two mutually compatible approaches which were investigated to address and mitigtate the AA interference issue. First, effects of increased PEDOT/fCNT deposition will be explored as a mechanism for achieving greater DA selectivity over AA. Second, modifications to the SWV waveform designed to minimize AA detection will be investigated, comprising application of a 0 V static potential prior to scanning.

2.2 Addressing *In Vitro* Calibrations

As is the case for all neurochemical sensing paradigms, proper interpretation of *in vivo* SWV measurements critically depends on the quality of constructed calibrations. SWV directly provides a measure of current, following extraction of the peak amplitude for the redox profile of a particular analyte. However this measure does not intrinsically provide useful information regarding the DA concentration at the local *in vivo* environment at the scan time. In order to correlate this metric with a specific concentration, it is necessary to construct a calibration curve, which represents the relationship exhibited by the particular sensor between the DA concentration and peak amplitude observed. In traditional *in vivo* SWV, these calibration curves are constructed following the recording by performing scans *in vitro* in artifical cerebrospinal fluid (aCSF) at increasing DA concentrations which span the concentration region of interest. Peak amplitudes may be extracted for each concentration and a calibration curve may be constructed by fitting a 1^{st} order regression to the peak vs. concentration data (Fig. 7).

The reliability of this calibration method may be questioned once the differences betwen aCSF and the *in vivo* recording environment are considered. aCSF poorly mimics numerous properties of the CNS parenchymal tissue, including electrochemical impedance, detailed chemical composition, poroelasticity, protein composition, presence of cellular elements and others. These significant discrepancies naturally lead to skepticism regarding the applicability of calibration curves constructed in aCSF to the interpretation of data recorded *in vivo*. It is currently unclear how these various discrepancies may lead to differences in electrode

sensitivity between the *in vivo* and *in vitro* environment. Thus, in the second portion of this work, these differences will be scrutinized and methods to construct a more representative *in vitro* calibration environment will be explored, in hopes of obtaining calibration curves which may be more confidently applied to *in vivo* recordings.

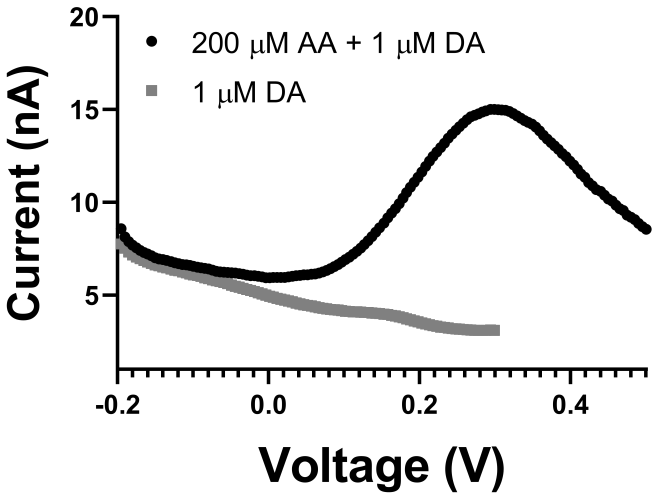

Figure 6: Representative ΔI traces from a CFE in artificial cerebrospinal fluid at supraphysiological [DA] (1 μM, grey) and the same [DA] with physiological [AA] (200μM). A small DA peak is observed at ∼0.15 V in the grey trace, which is rendered undetectable in the black trace due to the presence of a large and broad masking AA redox profile.

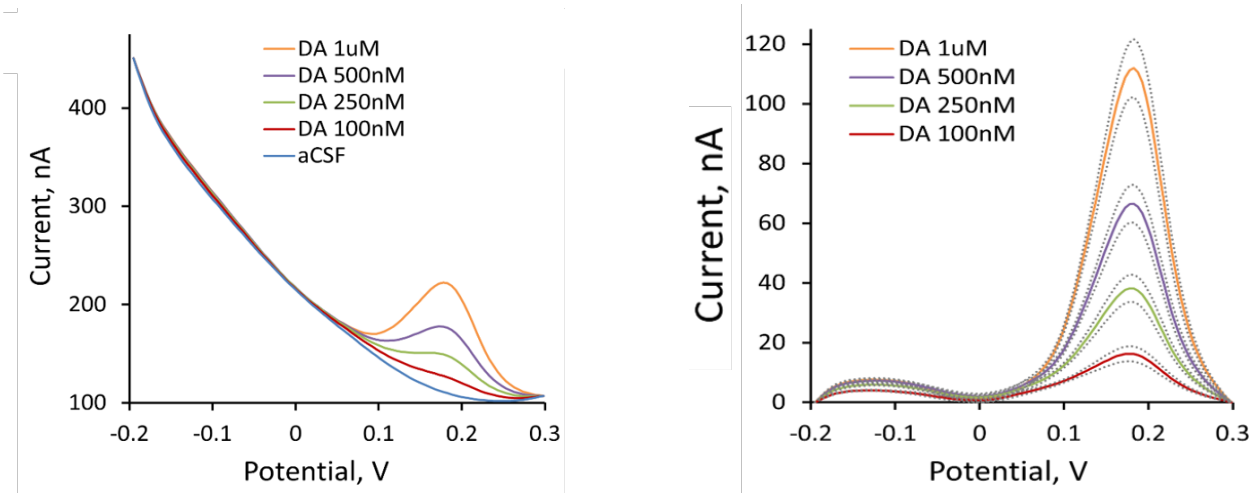

(a) (b)

Figure 7: (a) Representative DA calibration set performed *in vitro*. (b) Peak amplitudes extracted via baseline substraction. Linear regression is performed on the peak amplitude vs. concentration data.

3.0 PEDOT/fCNT for AA Signal Attenuation

The emergence of redox activity for a particular electrochemically active molecule during a SWV scan depends critically on two criteria. First, the redox potential of the species must exist within the boundaries of the scan, and second, the molecule must physically adsorb to the surface of the electrode to facilitate direct electron transfer during the redox reactions. Altering the boundaries of the SWV waveform may be considered in some regimes, but must be ruled out in the case of DA signal interference by AA. At bare CFEs, it is not possible to alter the boundaries due to the broad nature of the AA redox profile. At PEDOT/fCNT coated CFEs, it was found that the AA redox profile shifts negatively to be centered approximately at 0 V, in keeping with the theoretical predictions and early experimental investigation of AA oxidation [41]. Therefore at coated CFEs it is also not possible to alter the waveform boundaries in hopes of inducind DA redox activity without AA redox activity since the DA redox potential is greater than that of AA (in all cases AA redox activity will be induced if DA detection is desired). Therefore, waveform boundary alterations were not feasible and attention was drawn to methods by which AA adsorption may be reduced in hopes of attenuating AA redox currents in the measured signal.

At physiological pH of 7.4, AA ionizes into ascorbate with high dissociation constant, resulting in a stable structure which possesses a negative charge (Fig. 8) [42]. Due to the presence of negatively charged carboxylate groups in the PEDOT/fCNT coating, it was hypothesized that increased surface deposition would decrease the relative bulk proportion of AA near the surface of the electrode via electrostatic repulsion. In turn, this was predicted to decrease the amount of AA adsorbed to the surface of the electrode and ultimately reduce the AA oxidation signal present in the SWV scan. Thus, an inverse relationship was predicted between the extent of PEDOT/fCNT surface coating and the magnitude of the AA oxidation signal. However, given previous results from DA sensitivity analysis on PEDOT/fCNT coated CFEs, there remained uncertainty regarding the effects of a suspected increase in sensitivity to AA faradiac currents, which may be sufficient to overcome the beneficial effects of reduced surface adsorption. Ultimately the effects of reduced adsorption were predicted

to be greater.

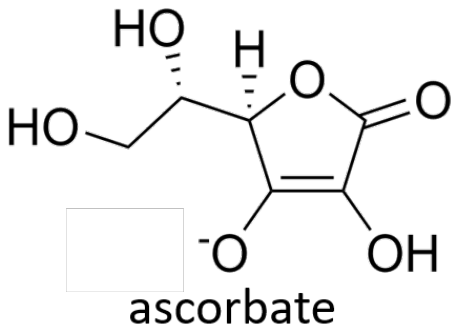

Figure 8: Ascorbic acid assumes its ionic form, ascorbate, at physiological pH 7.4.

3.1 Results

CFEs were prepared with 25, 100, and 200 mC/cm^2 PEDOT/fCNT deposition followed by DA and AA calibrations performed in aCSF for sensitivity analysis. Additional DA calibrations were performed in aCSF at 200μM AA to charaterize hypothesized mitigating effects of PEDOT/fCNT on AA-DA interference. From these calibrations, the 500 nM DA + 200μM AA scan was used to determine the ratio of DA:AA peak amplitudes and the extent of peak separation measured as the distance in volts within the scan between the peaks of the AA and DA redox profiles (see methods for details).

Contrary to hypothesized effects, AA sensitivity was found to increase significantly with increased PEDOT/fCNT deposition (Fig. 9a). Data sets obtained from the 25 mC/cm^2 CFE group were excluded from relative amplitude and peak separation analysis, as the DA and AA redox profile overlap was sufficient to prevent isolated quantification of the two individual peaks. It may be assumed that the effective peak separation is 0 V for the 25 mC/cm^2 CFE group, as this represents how the scans are treated in practice. Considering only the 100 and 200 mC/cm^2 groups, relative peak amplitude and peak separation was found to increase significantly with increased deposition (Fig. 9b,c). The hypothesized impact of

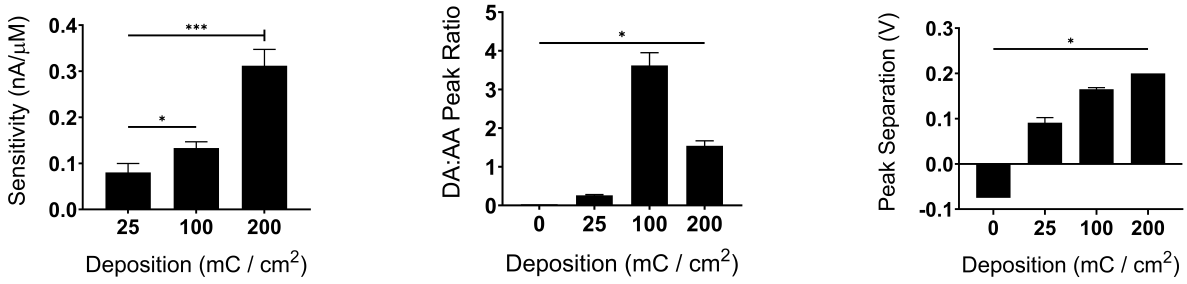

(a) (b) (c)

Figure 9: (a) AA detection sensitivity per deposition condition, calculated as the slope of the 1^{st} order regression to the extracted peak amplitudes vs. concentration data sets. Extending bars indicate SEM, $*$ indicates $p < 0.05$, and $***$ indicates $p < 0.0001$. (b) Relative peak amplitude per deposition condition, calculated as the ratio between DA and AA redox profile amplitudes. Extending bars indicate SEM, and $*$ indicates $p < 0.0005$. (c) Peak separation per deposition condition. $*$ indicates $p < 0.0000005$

PEDOT/fCNT on AA sensitivity was negated, but PEDOT/fCNT still exhibited useful peak separation effects for mitigating AA-DA interference, as greater separation indicates greater isolation of the redox profiles.

4.0 Waveform Modifications for AA Signal Attenuation

Although waveform truncation was ruled out as a possible strategy for addressing the interference between DA and AA redox profiles, an alternative voltammetric approach was devised in hopes of reducing presence of AA at the surface of the electrode during SWV scans. As previously mentioned, 100 mC/cm^2 PEDOT/fCNT coated CFEs exhibit AA oxidation profiles centered slightly below 0 V, in agreement with early theoretical predictions and experimental results [41]. The DA redox potential exists well above 0 V at ∼0.15 V. Thus, it is reasonably justified to assume that a 0 V static potential may be applied without affecting the ratio of DA to dopamin-o-quinone, the oxidation product of DA, at the electrode surface, which could have the adverse affect of reducing the DA signal. Therefore, it follows that a static potential at 0 V may be utilized to pre-oxidize AA near the electrode surface prior to SWV scanning.

Two effects were hypothesized to result from prolonged 0 V static potential application before SWV. In aqueous solution and under oxidation conditions, AA is oxidized to dehydroascorbate which then rapidly undergoes irreversible hydrolysis to diketogulonate (DKG) [41]. Therefore, applying 0 V at the electrode in the presence of AA was hypothesized to decrease local [AA] while increasing [DKG]. Over time, this would have the effect of developing an [AA] gradient from the bulk solution to the electrode surface which increases in length over time. As the duration 0 V application increases, the spatial [AA] distribution may reach a state in which a long distance must be travelled from the electrode surface to reach concentrations comparable to the bulk, with [AA] steadily increasing with distance. This would ultimately result in less [AA] near the electrode surface and additionally less locally available [AA] to replenish lost [AA] during a SWV scan.

Ultimately, it was hypothesized that 0 V static potential application prior to SWV would exhibit an inverse relationship between duration and AA peak amplitude. Potential effects on DA detection were unclear.

4.1 Results

CFEs were prepared with 100 mC/cm^2 PEDOT/fCNT deposition and SWV was performed in aCSF with 0 V static potential applied between scans for 1, 3, 5, 10, 20, 30, 60, and 120 s in 200 μM AA and 500 nM DA solutions to assess the effect of static potential application on redox profile amplitude. Additionally, AA and DA calibrations were performed for 0, 15, and 60 s durations to assess impact on sensitivity for each analyte.

Increased static potential application of 0 V was found to significantly attenuate the AA peak amplitude (Fig. 11). A minimum signal amplitude was reached at 60 s, after which no significant changes in the peak size were observed. Unexpectedly, the DA peak signal was found to increase significantly with increased static potential (Fig. 11). Durations past 120 s were not tested given design limitations on desired temporal resolution for this system.

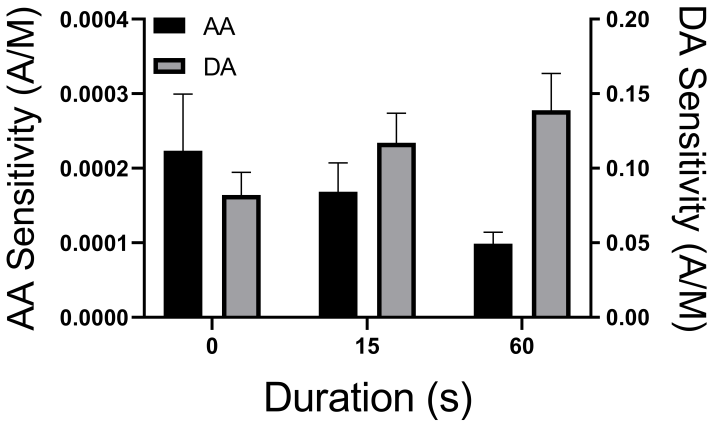

Figure 10: AA and DA sensitivity given particular duration of static 0 V potential application prior to SWV.

Sensitivity analysis was performed with three representative durations : 0, 15, and 60 s. 60 s was used as the maximum duration due to the absence of significant difference observed for longer durations. Despite an apparent decrease and increase in sensitivity observed for AA and DA respectively, static potential application was found to have no significant effect on AA or DA sensitivity, tested via Welch's T-Test (Fig. 10).

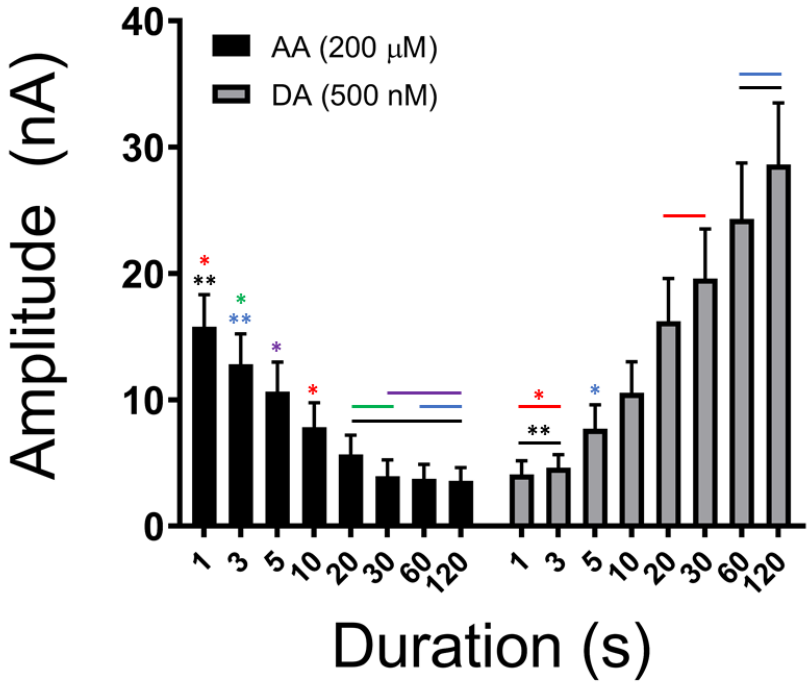

Figure 11: AA and DA signal amplitude for SWV following various durations of 0 V static potential. Extending bars indicate SEM, $*$ indicates $p < 0.05$, and $**$ indicates $p < 0.01$. All statistics were performed within the AA or DA group, not across.

5.0 Addressing In Vitro Calibrations

Traditional methods of obtaining calibration curves for electrochemical sensing techniques utilize solution-based calibration environments such as aCSF or PBS. However, these sustances poorly replicate important characteristics of the *in vivo* environment, such as electrochemical impedance, poroelasticity, protein content and others which may impact sensitivity and overall signal magnitude. Considering SWV application at PEDOT/fCNT coated CFEs, the possibility that the traditional *in vitro* calibration technique may be confounding interpretations of *in vivo* recordings first became apparent as discrepancies were observed in the overall magnitude of the SWV background current and in the magnitude of electrochemical impedance (Fig. 12).

Significant differences were observed in electrochemical impedance magnitude profiles obtained through electrochemical impedance spectroscopy for frequencies above 100 Hz, but differences in phase across all frequencies were insignificant. Additionally, *in vitro* and *in vivo* baseline SWV signals were found to exhibit a constant difference of approximately 1 μA across all points in the waveform. Although significance was not observed between the *in vitro* and *in vivo* CFE groups (Fig. 12d), this may be primarily attributed to high variability in the baseline signal across electrodes. Within-electrode differences were preserved for all electrodes studied, and large enough differences were exhibited to be considered a potential source of calibration confound. It was hypothesized that the intrinsic impedance difference between solution and neural tissue served as the source of SWV signal differences, and that if the calibration environment may be constructed to possess similar impedance to the *in vivo* situation, similar SWV scans would follow.

Two approaches were devised and tested for applicability in designing a novel *in vitro* calibration environment that sufficiently mimics *in vivo* impedance and SWV characteristics. Primary *in vivo* characteristics investigated comprise protein content and the combined poroelasticiy and bulk conductance properties.

5.1 Albumin Adsorption

Traditional calibration environments do not account for extensive *in vivo* extracellular protein content. Following implantation, it has been demonstrated that extracellular proteins coat the surface of implanted electrodes, in turn altering the electrochemical impedance and electrode resistance to faradaic charge transfer [43, 44]. Both of these electrochemical characteristics greatly influence SWV DA sensitivity, as the link between electrode impedance via PEDOT/fCNT coating has previously demonstrated (Fig. 5d). However, the effects due to protein adsorption have not been characterized for PEDOT/fCNT coated CFEs. Thus, it was hypothesized that protein adsorption may comprise a component of the total effect responsible for *in vivo* impedance and SWV signal differences.

To address this question, CFEs were prepared with 100 mC/cm^2 PEDOT/fCNT deposition and baseline impedance and SWV were collected in aCSF. Then, electrodes were exposed to 50 mg/ml bovine serum albumin in aCSF for 1 hr, allowing adsorption equilibrium to be reached. Albumin was utilized as a model adsorption protein due to its prevalence in the blood stream, high likelihood of exposure to an implanted microelectrode via blood vessel corruption, availability, and precedent in the literature [45, 46]. Subsequently, electrodes were transferred to fresh aCSF solution, and electrochemical impedance spectroscopy (EIS) and SWV were performed to assess protein adsorption impact on impedance and baseline SWV signal. Protein coatings were assumed to be stable during the solution transition due to extensive characterization of stability of these layers on various electrode substrates [47, 48, 49].

Contrary to expectation, no significant differences were observed in the impedance profiles or in the SWV baseline between the pre-adsorption and post-adsorption groups (Fig. 13).

5.2 Agarose Gels

An alternative approach to account for altered impedance and SWV signal considers the electrochemical properties of the bulk tissue rather than surface adsorption effects previously

covered. Specifically, neural tissue possesses poroelasticity, a characteristic which describes interactions between fluid and a solid medium consisting of pores and convoluted paths. However, solutions, such as aCSF, possess zero poroelasticity by definition. The relationship between poroelasticity and electrical conductance of a material has been well characterized, and thus connections between poroelastic properties of the recording medium, increased impedance and elevated SWV signal were considered [50]. Although the average impedance difference spectrum between *in vivo* and *in vitro* conditions posesses a imaginary components (Fig. 12c), a significant component of the spectrum is primarily real, suggesting that a simple bulk resistance achieved by altering poroelastic properties of the *in vitro* medium may be sufficient to account for the aforementioned discrepancies. However, this suggestion is contingent on the assumption that there is a direct link between impedance and SWV signal.

Agarose gels have been previously utilized to model bulk diffusion and poroelastic properties of neural tissue, and have successfully replicated CNS parenchymal tissue conductances at 0.6% concentration [51, 52]. Therefore, agarose gels were selected as a potential alternative medium in which post-measurement calibrations may be performed. It was hypothesized that *in vivo* conductance and poroelasticity characteristics may be replicated to achieve similar impedance *in vitro*, from which similar SWV profiles would naturally follow.

To address this hypothesis, 100 mC/cm^2 PEDOT/fCNT CFEs were prepared and baseline SWV and EIS scans in aCSF solution were performed. Agarose gels were prepared spanning the concentration range of 0.1% to 0.6%. Gels possessing concentrations above 0.6% were too stiff to allow for CFE implantation. After gels were allowed to set following initial fabrication, CFEs were implanted into the center of each gel concentration in turn, and EIS and SWV scans were performed. Additionally, preliminary data were collected to assess the effects of agarose concentration on DA sensitivity using a single 100 mC/cm^2 PEDOT/fCNT coated CFE. In this preliminary experiment, gels were prepared at 0.2%, 0.4%, and 0.6% at various DA concentrations, after which SWV scans were performed in each gel followed by sensitivity analysis (see methods for details).

Surprisingly, no significant differences in magnitude or phase were observed across agarose gel concentrations (Fig. 14a,b). Furthermore, no significant difference was observed in the

baseline SWV signal amplitude (data not shown). As a result, further analysis of SWV and agarose gel was not pursued, but preliminary data on DA sensitivity across agarose gel concentrations hinted at an apparent direct relationship between the two variables, although further testing is necessary for confirmation (Fig. 14a,b).

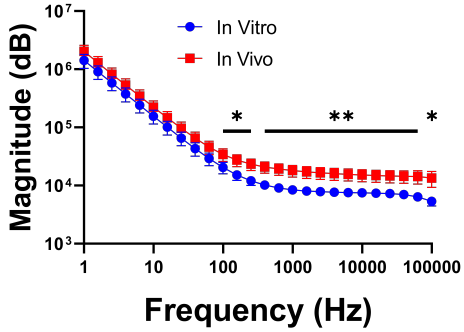

(a)

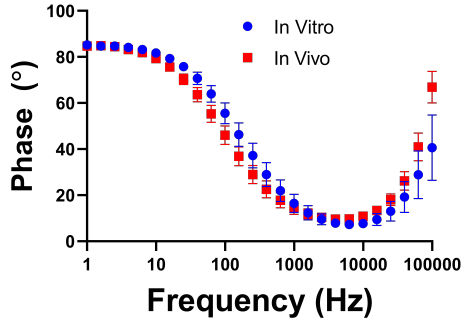

(b)

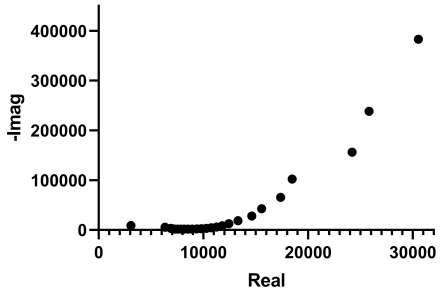

(c)

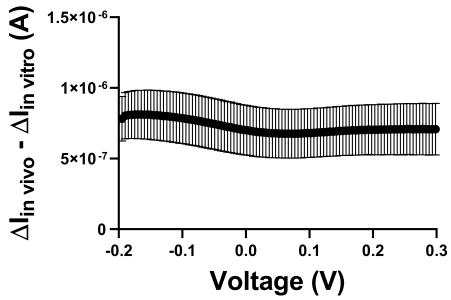

(d)

Figure 12: *In vivo* and *in vitro* impedance magnitude (a) and phase (b). $*$ signifies $p < 0.05$, and $**$ signifies $p < 0.01$. (c) Average impedance difference between *in vivo* and *in vitro* impedance. (d) SWV current difference ($n = 5$).

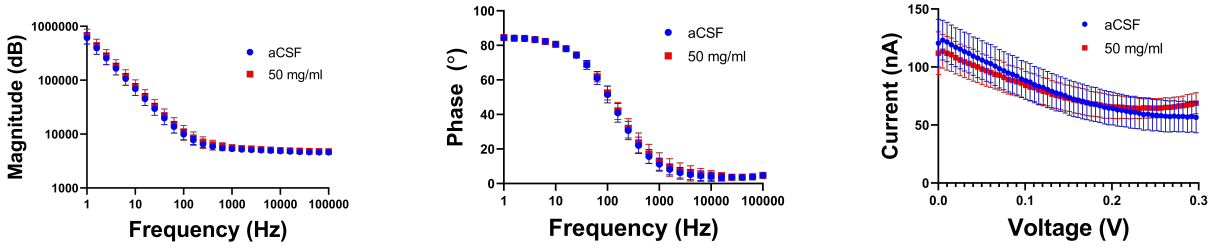

(a) (b) (c)

Figure 13: Impedance magnitude (a), phase (b) and baseline SWV signal (c) observed for pre-adsorption and post-adsorption PEDOT/fCNT CFEs. No significance was observed between groups for any of the three metrics.

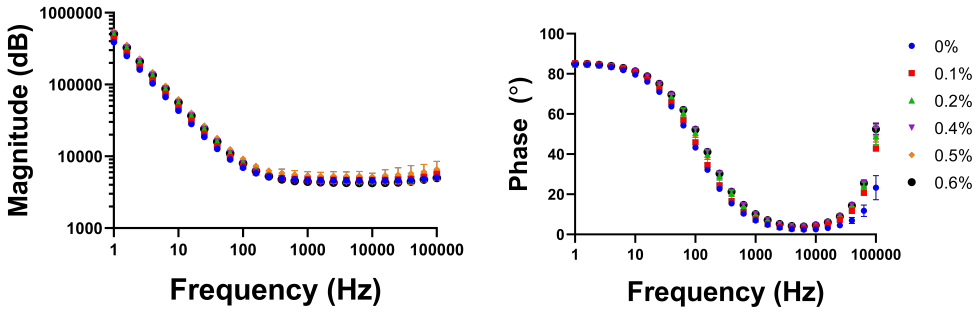

(a) (b)

Agarose Concentration	Dopamine Sensitivity (A/M)	Linear Regression R^2
0.2%	0.03253	0.987
0.4%	0.03798	0.992
0.6%	0.04015	0.994

(c)

Figure 14: Impedance magnitude (a), phase (b) observed for various agarose gel concentrations. No significant difference was observed betwen groups despite an apparent increase at high frequency phase. (c) Preliminary results for DA sensitivity in various agarose gel concentrations. An apparent increase was observed with increased concentration, and good fits were obtained for each calibration curve (high R^2).

6.0 Methods

6.1 Carbon Fiber Electrode Fabrication

Single carbon fibers (7 μm diameter, T650; Cytec Carbon Fibers LLC, Piedmont, SC, USA) were placed in the center of borosilicate glass capillaries (0.4 mm ID, 0.6 mm OD; A-M systems Inc., Sequim, WA, USA) and pulled to a fine tip (8 μm OD) using a vertical electrode puller (Narishige puller, Los Angeles, CA, USA). Electrode tips were sealed using low viscosity epoxy (Spurr Epoxy; Polysciences Inc., Warrington, PA, USA). The exposed carbon fibers were cut to 400 μm length as measured from the end of the pulled glass tip. Electrical connection to the carbon fiber was established by backfilling the capillary with liquid mercury and placing a nichrome wire into the end of the capillary (annealed nichrome; Goodfellow, Oakdale, PA, USA). Fully assembled electrodes were soaked in isopropanol for 10 minutes before proceeding [53].

6.2 PEDOT/fCNT Preparation and Deposition

Multi-walled carbon nanotubes (CNTs) were purchased (OD 2030 nm, ID 510 nm, length 1030 μm, purity > 95%, Cheap Tubes Inc., Brattleboro, VT, USA). 200 mg of CNTs were bath sonicated for 2 hr at ambient temperature in a 100 ml solution of 25 ml HNO_3 and 75 H_2SO_4 (Sigma-Aldrich Co., St. Louis, MO, USA) for surface carboxylation. The solution was then stirred at 50 °C for 12 h, then diluted to 1 L with DI water (Milli-Q, Millipore Co., Billerica, MA, USA). The mixture was left to settle for 2 hours, after which the supernatant was discarded. Carboxy-functionalized carbon nanotubes (fCNTs) were then transfered to a a SanakeSkin Dialysis Membrane (3.5k MWCO, 35mm diameter) and dialyzed for 48 hours in DI water. Water was renewed every 6-12 hours until a neutral pH was reached after the next 6-12 hour cycle. fCNTs were then transferred to a crystallization dish and bath sonicated for 2 hrs, after which a final 6-12 hour period of dialysis was performed. fCNTs

were extracted via Rotovap [37].

EDOT/fCNT polymerization solution was prepared via mixing 1.5 mg fCNTs with 1.5 mL DI water followed by bath sonication for 2 min. 1.5 μL 3,4-ethylenedioxythiophene (EDOT) (Sigma-Aldrich, St. Louis, MO, USA) was added to the mixture, followed by 2 min vortex mixing and 45 min probe sonication using a 2 s pulse 1 s rest function. Final solutions were stored at 1.6 °C for $>$ 10 min prior to polymerization.

Polymerization was conducted using a 3 electrode setup with a Ag/AgCl reference electrode, Pt counter electrode, and pre-fabricated bare CFE as the working electrode submerged in EDOT/fCNT solution. Chronocoulombetric coating were performed under potentiostatic control at 0.9 V (Metrohm Autolab, PGSTAT128N). Coating was terminated once a pre-calculated charge cutoff was reached. Charge cutoffs were calculated via considering electrode surface area and desired charge density (100 mC/cm^2). Surface area was obtained by measuring exposed carbon fiber length and applying a cylindrical approximation.

6.3 Dopamine and Ascorbic Acid Calibrations

All calibrations were performed under potentiostatic control using a SWV waveform at 25 HZ, 0.05 V modulation amplitude, and 0.005 V step size, from -0.2 V to 0.4 V (Metrohm Autolab, PGSTAT128N). Potential was held at 0 V between scans for durations specified by the type of calibration being performed. DA and AA calibrations were performed in artificial cerebrospinal fluid (aCSF, 142 mM NaCl, 1.2 mM CaCl2, 2.7 mM KCl, 1.0 mM MgCl2, 2.0 mM NaH2PO4, pH 7.4). Detection peaks for both analytes were extracted by first estimating the peak boundaries via linear baseline approximation and then performing a 2^{nd} order regression using 20 data points (10 on either side of the estimated peak). Peak values were taken as the maximum difference between the scan and regression fit within the peak region. Electrode sensitivity was determined by computing the 1^{st} order linear regression to the peak vs concentration data and taking the slope, representing the estimated proportionality constant between peak amplitude and [DA] or [AA]. DA calibrations (0 nM, 100 nM, 250 nM, 500 nM, 1 μM) and AA calibrations (0 nM, 100 μM, 200 μM, 300μM) were

performed by collecting scans in aCSF the specified analyte concentrations. DA calibrations were also performed in the presence of 200 μM AA to further characterize selectivity. All data were analyzed in MATLAB (Mathworks, MA). Statistical significance tests were performed using Welch's 2-sample T-Test.

6.4 In Vivo Measurements

For each *in vivo* recording, a male Sprague Dawley rat (350-450 g, Charles River, Wilmington, MA, USA) was anesthetized with 2% isoflurane by volume (Henry Schein, Melville, NY, USA) and positioned in a stereotaxic head restraint to flat skull orientation. The skull and dura were removed to allow for the positioning of a single PEDOT/fCNT coated CFE into the dorsal striatum (2.5 mm lateral to bregma, 0.42 mm anterior to bregma, 5 mm below the cortical surface) and two additional holes were bored into the skull to accommodate the positioning of a Ag/AgCl reference electrode contralaterally to the CFE and a bone screw counter electrode caudally to the reference. Electrochemical impedance spectroscopy was applied immediately following implantation, and SWV (waveform detailed above) was then applied over a 75-minute period. Upon reaching the predetermined experimental endpoint, the CFE was explanted for post-calibration (calibration detailed above) and the animal was sacrificed. All data were analyzed in MATLAB (Mathworks, MA). Statistical significance tests were performed using Welch's 2-sample T-Test, and p-values greater than 0.05 were considered insignificant.

6.5 Albumin Adsorption

Bovine serum albumin (BSA) (Sigma Aldrich, St. Louis, MO, USA) was dissolved in 20 ml aCSF (preparation described in calibration section) for a final concentration of 50 mg/ml. Electrochemical impedance spectroscopy (EIS) and SWV was collected in aCSF at 100 mC/cm^2 PEDOT/fCNT coated CFEs, followed by 1 hr soaking in the prepared BSA

solution. Then, CFEs were moved to a fresh aCSF solution for a second collection of SWV and EIS. All data were analyzed in MATLAB (Mathworks, MA). Statistical significance tests were performed using Welch's 2-sample T-Test, and p-values greater than 0.05 were considered insignificant.

6.6 Agarose Gel Experimentation

0.1% to 0.6% agarose gels were prepared via mixing agarose (Sigma-Aldrich, St. Louis, MO, USA) in 250 mL aCSF followed by 1000 W microwave on high power for 2 min. Heated mixtures were then cast into 6-plate wells. aCSF/DA solutions were added immediately following casting for gels to be prepared at specified [DA] for calibrations. All mixtures were allowed to gel at room temperature. Once the gels settled, CFEs coated to 100 mC/cm^2 were inserted for EIS and SWV measurements. All data were analyzed in MATLAB (Mathworks, MA). Statistical significance tests were performed using Welch's 2-sample T-Test, and p-values greater than 0.05 were considered insignificant.

7.0 Discussion

Increased AA sensitivity and relative AA signal to DA signal due to increased PEDOT/fCNT deposition indicates that PEDOT/fCNT sensitivity to charge transfer exhibited stronger effects than the expected primary effect of electrostatic repulsion of AA from the surface. It may be possible that electrostatic repulsion was not achieved due to ambient cationic species accumulating on the surface to cancel the intrinsic fCNT negative charge, although further and more precise work is required to determine the specific mechanism responsible for this effect.

Although increased PEDOT/fCNT deposition resulted in increased AA sensitivity and decreased DA:AA peak ratio, this method may still be utilized to reduce AA interference. This may be primarily inferred through the peak separation analysis. As long as sufficient peak separation is maintained, relative sensitivities and peak amplitudes are irrelevant, as sufficient separation enables independent quantification. In this sense, PEDOT/fCNT has been greatly successful in converting electrodes previously incompatible with simultaneous DA and AA quantification into electrodes capable of resolving both signals with reasonable separation. However, through investigation into *in vivo* application, it has been discovered that coating density must be limited to 100 mC/cm^2 to avoid issues of extensive non-faradiac signals. In the case of 150 and 200 mC/cm^2 coatings, non-faradaic current decays possessed time constants too large for faradaic currents to be effectively sampled using the developed SWV waveform. Therefore, at present *in vivo* application is limited to 100 mC/cm^2 PEDOT/fCNT coated electrodes. Even so, significant peak separation is observed at that coating condition, and applications *in vivo* in the dorsal striatum of anesthetized rats have succesfully resolved basal DA signals, even without the necessary addition of waveform alterations.

Nonetheless, it is clear that 0 V static potential application provides multiple benefits for *in vitro* SWV at PEDOT/fCNT coated CFEs. For further mitigated AA interference, 0 V may be held for 15s between scans, maintaining a sampling resolution higher than that of FSCAV. This also serves the additional benefit of significantly increasing DA signal ampli-

tude. Although this effect does not translate to enhanced sensitivity, greater amplitudes provide easier and more reliable quantification via elevated signal-to-noise ratio. Increased DA amplitude is thought to be the primary result of electrostatic interaction with carboxylate groups on the fCNTs. At physiological pH, DA possesses a positive charge. Therefore, by holding at 0 V, all non-faradaic charging dynamics are removed from the system and ambient DA is able to interact passively with the negatively charged fCNTs without an external voltage drive. This would have the effect of pre-adsorbing DA to the surface due to electrostatic attraction, such that during the scan the local [DA] is elevated relative to the bulk solution.

Regarding the inability of agarose gels to replicate *in vivo* conditions, it is hypothesized that this result is primarily due to differences in scale between the porosity of the gel and the size of the electrode. Although the gel may exhibit bulk poroelastic and conductive properties similar to that of neural tissue, it may be possible that at the scale of the CFE surface, the environment is indistinguishable from that of a simple aCSF solution due to relatively large pore size. It may also be possible that the gels behave as aCSF solutions for currents below a particular threshold, since the effects of conductance may only manifest in the case of bulk currents traversing the entire medium. In the case of SWV, currents are largely confined to the immediate region surrounding the electrode and thus the conductance effects of aCSF reported previously may not be observed [51, 52].

The lack of protein adsorption effects on impedance or SWV were initially surprising but may hint at a valuable protection mechanism exhibited by PEDOT/fCNT coatings. Specifically, the PEDOT/fCNT coating exhibits a highly porous morphology (Fig. 5b). This morphology may serve as a size exclusion layer for the electrode surface, allowing small molecules, such as ions, to pass unperturbed to the surface while proteins remain aggregated at the surface. This assumes that the BSA adsorption layer does not form tight connections between adjacent proteins. This suggestion is somewhat supported by the insignificant effects on impedance and SWV magnitude. However, it is suspected that the accumulation of a more complex biofilm *in vivo* over long-term *in vivo* recordings would eventually impact DA sensitivity. One simple mechanism by which this may occur is that biofilm accumulation could reduce the available PEDOT/fCNT surface for direct DA interaction, thus lowering

redox activity throughout a scan and in turn reducing sensitivity.

Preliminary data from the agarose gel DA sensitivity experiments indicate that the presupposed link between sensitivity and impedance may not be founded. There appears to be a slight increase in sensitivity as agarose concentration is increased, but additional replicates are necessary to confirm a relationship.

8.0 Conclusion

This work has demonstrated that PEDOT/fCNT may be used to facilitate DA selectivity over AA, and that further selectivity and increases in DA detection amplitude may be achieved through application of a 0 V static potential duration prior to SWV scans. Through considering these two alterations to the originally conceived neurochemical sensing system, *in vivo* application may be realized for successful resolution of basal DA signalling at high temporal resolution. However, this technique still suffers, as do all electrochemical sensing techniques, from discrepancies in *in vitro* calibration conditions and the *in vivo* environment. Initial experiments on the design of a suitable *in vitro* calibration platform have ruled out two previously promising approaches and suggest possible robustness of SWV to protein adsorption. Therefore, alternative methods must be explored to account for these discrepancies. Nonetheless, this work represents a major step forward in realizing a powerful basal DA sensing tool for the neurosciences and bioengineering.

9.0 Future Directions

In future work, it will be necessary to determine the generalizability of AA interference mitigating techniques to metallic site MEAs. Additionally, chronic *in vivo* recordings may be performed to assess long-term recording quality and interference characteristics over time. In hopes of achieving a more reliable *in vitro* calibration environment, alternative aqueous gels may be explored which possess smaller pore size compared to aCSF, and different proteins may be tested for modelling *in vivo* protein adsorption. Additionally, electrical circuits attached between the working electrode and potentiostat may be explored as a precise mechanism by which *in vitro* impedance may be controlled and manipulated [54]. In addition to assessing impedance and baseline SWV magnitude, DA sensitivity may also be assessed for each of the conditions tested to determine if the supposed links between impedance, SWV signal amplitude, and sensitivity are justified.

10.0 Appendix

10.1 Circuit Modelling for In Vitro Calibrations

An alternative approach for simulating *in vivo* impedance during *in vitro* calibrations was demonstrated by Meunier et al for fast-scan cyclic voltammetry at CFEs [54]. The method they developed comprises connecting an electrical circuit in series between the potentiostat and the working electrode in order to alter the total impedance of the *in vitro* calibration setup (Fig. 16).

Preliminary experimentation demonstrated that connecting resistors to the working electrode during SWV scans in aCSF resulted in increased baseline SWV signal, although adapting this method for electrodes following *in vivo* recordings revealed that resistors were insufficient to recapture the *in vivo* baseline.

Adaptation of this general method was employed for Ag electrode microelectrode sites used for *in vivo* cortical current-controlled stimulation in Sprague Dawley rats. A Randall's circuit was constructed and attached in series between the potentiostat and electrode *in vitro* in aCSF following *in vivo* stimulation to accurately replicate the *in vivo* stimulation voltage waveform Ṗreliminary success of this method for correcting the *in vitro* calibration environment suggests that more complex circuit configurations than single resistors, such as the Randall's circuit employed here, could result in the replication of *in vivo* SWV baseline profiles during *in vitro* calibrations.

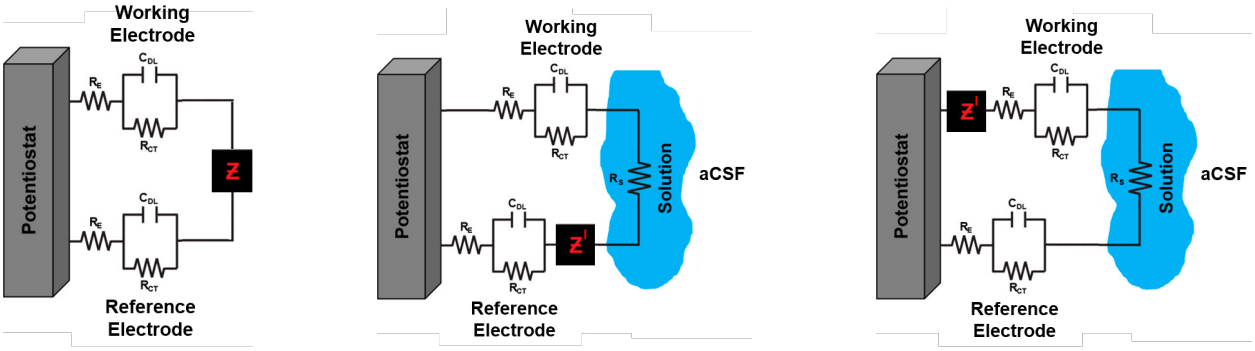

(a) (b) (c)

Figure 15: (a) Equivalent circuit model of an *in vivo* electrochemical detection platform adapted from Meunier et al., depicting the working electrode and reference electrodes as Randall's circuits, and the tissue impedance as a generalized impedance element Z. (b) Z is parsed into Z' and R_s, where $Z' + R_s = Z$ and R_s represents the solution resistance of aCSF. (c) Impedance elements in series add linearly, so moving Z' between the potentiostat and working electrode does not alter the total circuit impedance. This allows the experimentalist to connect a physical electrical circuit with impedance Z' to the *in vitro* calibration setup in order to equate the total impedance with that of the *in vivo* environment.

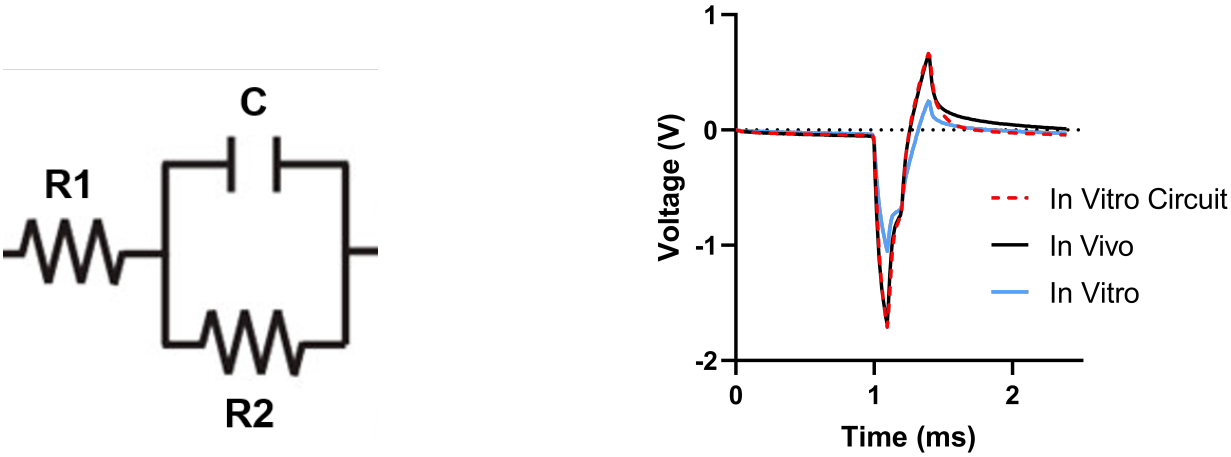

(a) (b)

Figure 16: (a) Randall's circuit employed for *in vitro* correction (parameter values $R1 = 122k\Omega, R2 = 100k\Omega, C = 300pF$). (b) *In vivo*, *in vitro*, and *in vitro* corrected (with Randall's circuit attached) voltage responses to the stimulation waveform. The corrected response corresponds closely with the response obtained *in vivo*.

11.0 References

[1] P. Greengard J.A. Girault. "The Neurobiology of Dopamine Signaling". In: *Archives of Neurology* 61.5 (2004), pp. 641–644. DOI: 10.1001/archneur.61.5.641.

[2] D.J. Brooks. "Functional Imaging Studies on Dopamine and Motor Control". In: *Journal of Neural Transmission* 108.11 (2001), pp. 1283–1293. DOI: 10.1007/s0070-20100005.

[3] X. Liu and A.E. Herbison. "Dopamine Regulation of Gonadotropin-Releasing Hormone Neuron Excitability in Male and Female Mice". In: *Endocrinology* 154.1 (2013), pp. 340–350. DOI: 10.1210/en.2012-1602.

[4] N.B. Urban et al. "Imaging human reward processing with positron emission tomography and functional magnetic resonance imaging". In: *Psychopharmacology* 221.1 (2012), pp. 66–77. DOI: 10.1007/s00213-011-2543-6.

[5] D. Calu D. Caprioli and Y. Shaham. "Loss of Phasic Signaling: a New Addiction Marker?" In: *Nature Neuroscience* 17.5 (2014), pp. 644–646. DOI: PMID:24883455.

[6] J.J. Clark M. Wanat I. Willuhn and P.E. Phillips. "Phasic dopamine release in appetitive behaviors and drug addiction". In: *Current Drug Abuse Review* 2.2 (2010), pp. 195–213. DOI: PMID:19630749.

[7] W. Schultz. "Predictive Reward Signal of Dopamine Neurons". In: *Journal of Neurophysiology* 80.1 (1998), pp. 1–27. DOI: 10.1152/jn.1998.80.1.1.

[8] W. Schultz. "Multiple Dopamine Functions at Different Time Courses". In: *Annual Review of Neuroscience* 30 (2007), pp. 259–288. DOI: 10.1146/annurev.neuro.28.061604.135722.

[9] P. Belujon and A.A. Grace. "Dopamine System Dysregulation in Major Depressive Disorders". In: *The International Journal of Neuropsychopharmacology* 20.12 (2017), pp. 1036–1046. DOI: 10.1093/ijnp/pyx056.

[10] E.H. Cook et al. "Association of attention-deficit disorder and the dopamine transporter gene". In: *American Journal of Human Genetics* 56.4 (1995), pp. 993–998. DOI: PMID:7717410.

[11] Y. Agrid P. Damier E.C. Hirsch and A.M. Graybiel. "The substantia nigra of the human brain. II. Patterns of loss of dopamine-containing neurons in Parkinson's disease". In: *Brain* 112.8 (1999), pp. 1437–1448. DOI: PMID:10430830.

[12] A.A. Grace. "Dysregulation of the dopamine system in the pathophysiology of schizophrenia and depression". In: *Nature Reviews* 17.8 (2016), pp. 524–532. DOI: 10.1038/nrn.2016.57.

[13] J.M.R Delgado et al. "Dialytrode for long term intracerebral perfusion in awake monkeys". In: *Arch Int Pharmacodyn Ther* 198.1 (1972), pp. 9–21. DOI: PMID:4626478.

[14] U. Ungerstedt and C. Pycock. "Functional correlates of dopamine neurotransmission". In: *Bull Schweitz Akad Med Wiss* 30.1-3 (1974), pp. 44–55. DOI: PMID:4371656.

[15] V. Chefer et al. "Overview of brain microdialysis". In: *Current Protocols in Neuroscience* (2009). DOI: 10.1002/0471142301.ns0701s47.

[16] H. Gu et al. "In Vivo Monitoring of Dopamine by Microdialysis with 1 min Temporal Resolution Using Online Capillary Liquid Chromatography with Electrochemical Detection". In: *Analytical Chemistry* 87.12 (2015), pp. 6088–6094. DOI: 10.1021/acs.analchem.5b00633.

[17] G.W. Cheng et al. "On-line Microdialysis Coupled with Liquid Chromatography for Biomedical Analysis". In: *Journal of Chromatographic Science* 47.8 (2009), pp. 624–630. DOI: PMID:19772738.

[18] J. Kehr. "Determination of glutamate and aspartate in microdialysis samples by reversed-phase column liquid chromatography with fluorescence and electrochemical detection". In: *Journal of Chromatography B Biomedical Science Applications* 708.1-2 (1998), pp. 27–38. DOI: PMID:9653943.

[19] A.V. Eeckhaut et al. "The absolute quantification of endogenous levels of brain neuropeptides in vivo using LC-MS/MS". In: *Bioanalysis* 3.11 (2011), pp. 1271–1285. DOI: 10.4155/bio.11.91.

[20] O.S. Mabrouk et al. "Microdialysis and mass spectrometric monitoring of dopamine and enkephalins in the globus pallidus reveal reciprocal interactions that regulate movement". In: *Journal of Nuerochemistry* 118.1 (2011), pp. 24–33. DOI: 10.1111/j.1471-4159.2011.07293.x.

[21] R.A. Saylor et al. "A review of microdialysis coupled to microchip electrophoresis for monitoring biological events". In: *Journal of Chromatography A* 1382 (2015), pp. 48–64. DOI: 10.1016/j.chroma.2014.12.086.

[22] K.T. Ngo et al. "Monitoring Dopamine Responses to Potassium Ion and Nomifensine by in vivo Microdialysis with Online Liquid Chromatography at One-Minute Resolution". In: *ACS Chemical Neuroscience* 8.2 (2017), pp. 329–388. DOI: 10.1021/acschemneuro.6b00383.

[23] K.M. Nestbitt et al. "Pharmacological mitigation of tissue damage during brain microdialysis". In: *Analytical Chemistry* 85.17 (2013), pp. 8173–8179. DOI: 10.1021/ac401201x.

[24] T.K.D.Y Kozai et al. "Brain tissue responses to neural implants impact signal sensitivity and intervention strategies". In: *ACS Chemical Neuroscience* 6.1 (2014), pp. 48–67. DOI: doi:10.1021/cn500256e.

[25] V. Bassareo et al. "Monitoring dopamine transmission in the rat nucleus accumbens shell and core during acquisition of nose-poking for sucrose". In: *Behavioral Brain Research* 287 (2015), pp. 200–206. DOI: 10.1016/j.bbr.2015.03.056.

[26] C.W. Atcherly et al. "Fast-Scan Controlled-Adsorption Voltammetry for the Quantification of Absolute Concentrations and Adsorption Dynamics". In: *Langmuir* 29.48 (2013), pp. 14885–14892. DOI: 10.1021/la402686s.

[27] C.E. John and S.R. Jones. "Fast Scan Cyclic Voltammetry of Dopamine and Serotonin in Mouse Brain Slices". In: *Frontiers in Neuroengineering* (2007). DOI: PMID:21204393.

[28] L.J. May R.M Wightman and A.C. Michael. "Detection of Dopamine Dynamics in the Brain". In: *Analytical Chemistry* 60.13 (1988), 769A–779A. DOI: 10.1021/ac00164a001.

[29] Y. Oh et al. "Monitoring In Vivo Changes in Tonic Extracellular Dopamine Level by Charge-Balancing Multiple Waveform Fast-Scan Cyclic Voltammetry". In: *Analytical Chemistry* 88.22 (2016), pp. 10962–10970. DOI: 10.1021/acs.analchem.6b02605.

[30] C.W. Atcherly et al. "The coaction of tonic and phasic dopamine dynamics." In: *Chemical Communications* 51.12 (2015), pp. 2235–2238. DOI: 10.1039/c4cc06165a.

[31] G.T. Kovacs et al. "Silicon-substrate microelectrode arrays for parallel recording of neural activity in peripheral and cranial nerves". In: *IEEE Translational Biomedical Engineering* 41.6 (1994), pp. 567–577.

[32] M.K. Zachek. "Microfabricated FSCV-compatible microelectrode array for real-time monitoring of heterogeneous dopamine release". In: *Analyst* 135.7 (2010), pp. 1556–1563. DOI: 10.1039/c0an00114g.

[33] M.K. Zachek. "Electrochemical dopamine detection: Comparing gold and carbon fiber microelectrodes using backgrounds substracted fast scan cyclic voltammetry". In: *Journal of Electroanalytical Chemistry* 613.1-2 (2008), pp. 113–120. DOI: 10.1016/j.jelechem.2007.11.007.

[34] J.G. Osteryoung and R.A. Osteryoung. "Square wave voltammetry". In: *Analytical Chemistry* 57.1 (1985), pp. 101–110. DOI: 10.1021/ac00279a004.

[35] Y. Oh et al. "Tracking tonic dopamine levels in vivo using multiple cyclic square wave voltammetry". In: *Biosensors and Bioelectronics* 121 (2018), pp. 174–182. DOI: 10.1016/j.bios.2018.08.034.

[36] A.J. Bard and L.R. Faulkner. *Electrochemical Methods. Fundamentals and Applications*. 2nd ed. Wiley, 2007.

[37] N.A. Alba et al. "*In Vivo* Electrochemical Analysis of a PEDOT/MWCNT Neural Electrode Coating". In: *Biosensors* 5.4 (2015), pp. 618–646. DOI: 10.3390/bios5040618.

[38] T.D. Kozai et al. "Chronic in Vivo Evaluation of PEDOT/CNT for Stable Neural Recordings". In: *IEEE Translational Biomedical Engineering* 63.1 (2016), pp. 111–119. DOI: 10.1109/TBME.2015.2445713.

[39] I. Bokkon and I. Antal. "Schizophrenia: Redox Regulation and Volume Neurotransmission". In: *Current Neuropharmacology* 9.2 (2011), pp. 289–300. DOI: 10.2174/157015911795596504.

[40] J.A. Johnson et al. "Measurement of Basal Neurotransmitter Levels Using Convolution-Based Non-fara- daic Current Removal". In: *Analytical Chemistry* 90.12 (2018), pp. 7181–7189. DOI: 10.1021/acs.analchem.7b04682.

[41] H. Borsook and G. Keightley. "Oxidation-Reduction Potential of Ascorbic-Acid (Vitamin C)". In: *Proc Natl Acad Sci USA* 19.9 (1933), pp. 875–878. DOI: PMCID:PMC1086204.

[42] US National Library of Medicine. *Toxicology Data Network*. 2010. URL: https://toxnet.nlm.nih.gov/cgi-bin/sis/search2/r?dbs+hsdb:@term+@rn+@rel+50-81-7 (visited on 04/05/2019).

[43] S.E. Moulton et al. "Investigation of protein adsorption and electrochemical behavior at a gold electrode". In: *Journal of Colloid and Interface Science* 261.2 (2003), pp. 312–319. DOI: 10.1016/S0021-9797(03)00073-0.

[44] A.J. Downard and A.D. Roddick. "Protein adsorption at glassy carbon electrodes: The effect of covalently bound surface groups". In: *Electroanalysis* 7.4 (1995), pp. 376–378. DOI: 10.1002/elan.1140070414.

[45] S. Sommakia et al. "Effects of adsorbed proteins, an antifouling agent and long-duration DC voltage pulses on the impedance of silicon-based neural microelectrodes". In: *Conf Proc IEEE Eng Med Biol Soc* (2009), pp. 7139–42. DOI: 10.1109/IEMBS.2009.5332456.

[46] A. Campbell and C. Wu. "Chronically implanted intracranial electrodes: tissue reaction and electrical changes". In: *Micromachines (Basel)* 9.9 (2018), p. 430. DOI: 10.3390/mi9090430.

[47] D.R. Jackson et al. "Electrochemical studies of the adsorption behavior of serum proteins on titanium". In: *Langmuir* 16.12 (2000), pp. 5449–5457. DOI: 10.1021/la991497x.

[48] V. Hlady and J. Bujis. "Protein adsorption on solid surfaces". In: *Curr Opin Biotechnol* 7.1 (2012), pp. 72–77. DOI: PMCID:PMC3262180.

[49] J. Selvakumaran. "Protein adsorption on materials for recording sites on implantable microelectrodes". In: *J Mater Sci Mater Med.* 19.1 (2007), pp. 143–51. DOI: 10.1007/s10856-007-3110-x.

[50] O. Invanchenko et al. "Experimental techniques for studying poroelasticity in brain phantom gels under high flow microinfusion". In: *J. Biomech Eng* 132.5 (2010). DOI: 10.1115/1.4001164.

[51] Z.J. Chen et al. “A realistic brain tissue phantom for intraparenchymal infusion studies”. In: *Journal of Neurosurgery* 101.2 (2004), pp. 314–322. DOI: 10.3171/jns.2004.101.2.0314.

[52] M.A. Kandadai et al. “Comparison of electrical conductivities of various brain phantom gels: Developing a ’Brain Gel Model’”. In: *Mater Sci Eng C Mater Biol Appl* 32.8 (2013), pp. 2664–2667. DOI: 10.1016/j.msec.2012.07.024.

[53] I.M. Taylor et al. “Enhanced Dopamine Detection Sensitivity by PEDOT/Graphene Oxide Coating on in vivo Carbon Fiber Electrodes”. In: *Biosens Bioelectron* 89.1 (2016), pp. 400–410. DOI: 10.1016/j.bios.2016.05.084.

[54] C.J. Meunier et al. “The Background Signal as an In Situ Predictor of Dopamine Oxidation Potential: Improving Interpretation of Fast-Scan Cyclic Voltammetry Data”. In: *ACS Chemical Neuroscience* 8.2 (2017). DOI: 10.1021/acschemneuro.6b00325.